







EMC is required for biogenesis of Xport-A, an essential chaperone of Rhodopsin-1 and the TRP channel

Catarina J Gaspar^{1,2} , Lígia C Vieira^{1,†}, Cristiana C Santos¹ , John C Christianson³ , David Jakubec⁴, Kvido Strisovsky⁴ , Colin Adrain^{2,5,*}  & Pedro M Domingos^{1,**,†} 

Abstract

The ER membrane protein complex (EMC) is required for the biogenesis of a subset of tail anchored (TA) and polytopic membrane proteins, including Rhodopsin-1 (Rh1) and the TRP channel. To understand the physiological implications of EMC-dependent membrane protein biogenesis, we perform a bioinformatic identification of *Drosophila* TA proteins. From 254 predicted TA proteins, screening in larval eye discs identified two proteins that require EMC for their biogenesis: fan and Xport-A. Fan is required for male fertility in *Drosophila* and we show that EMC is also required for this process. Xport-A is essential for the biogenesis of both Rh1 and TRP, raising the possibility that disruption of Rh1 and TRP biogenesis in EMC mutants is secondary to the Xport-A defect. We show that EMC is required for Xport-A TMD membrane insertion and that EMC-independent Xport-A mutants rescue Rh1 and TRP biogenesis in EMC mutants. Finally, our work also reveals a role for Xport-A in a glycosylation-dependent triage mechanism during Rh1 biogenesis in the endoplasmic reticulum.

Keywords ER membrane protein complex; Rh1; tail anchored proteins; TRP; Xport-A

Subject Categories Membranes & Trafficking

DOI 10.15252/embr.202153210 | Received 6 May 2021 | Revised 26 October 2021 | Accepted 10 November 2021 | Published online 17 December 2021

EMBO Reports (2022) 23: e53210

Introduction

Membrane proteins comprise ~30% of the eukaryotic proteome and confer many essential functions to biological membranes (Wallin & Von Heijne, 1998; Fagerberg *et al*, 2010). These proteins contain

hydrophobic transmembrane domains (TMDs) that must be inserted into the membrane of the endoplasmic reticulum (ER) through evolutionarily conserved molecular machineries. The vast majority of membrane proteins are inserted into the ER membrane through the co-translational pathway, in which proteins containing signal peptides or TMDs are recognised by the signal recognition particle as they emerge from the ribosomes. Eventually, the ribosome-nascent chain complex is delivered to the Sec61 translocon, where membrane insertion takes place (Guna & Hegde, 2018).

The co-translational insertion pathway is the predominant mechanism for membrane protein insertion, but it is unable to deal with the biogenesis of a specific class of membrane proteins called tail anchored (TA) proteins, which lack a signal peptide and contain a single TMD at their C-terminus (Kutay *et al*, 1993). Consequently, their TMD remains shielded inside the ribosomal tunnel until the termination codon is reached, and TMD recognition can only occur post-translationally (Hegde & Keenan, 2011). Accordingly, TA proteins utilise a dedicated conserved TMD recognition complex (TRC) pathway, which facilitates the targeted release of these proteins into the ER in eukaryotic cells, in a post-translational manner (Stefanovic & Hegde, 2007). The crucial component of this pathway is the ATPase TRC40 (or in yeast Get3), which captures and shields TMDs of TA proteins (Stefanovic & Hegde, 2007; Schuldiner *et al*, 2008; Mateja *et al*, 2015), until they are released to a receptor complex composed of WRB-CAML (yeast Get1-Get2), which mediates TMD insertion into the ER membrane (Mariappan *et al*, 2011; Stefer *et al*, 2011). Structural and biochemical studies have shown that this pathway displays a preference for TMDs of high hydrophobicity (Wang *et al*, 2010; Rao *et al*, 2016; Guna *et al*, 2018).

Recently, the ER membrane protein complex (EMC) was identified as an insertase for TA proteins with TMDs of moderate to low hydrophobicity (Guna *et al*, 2018; Tian *et al*, 2019; Volkmar *et al*, 2019). The EMC is a highly conserved, multi-subunit protein

¹ Instituto de Tecnologia Química e Biológica da Universidade Nova de Lisboa (ITQB-NOVA), Oeiras, Portugal

² Membrane Traffic Lab, Instituto Gulbenkian de Ciência (IGC), Oeiras, Portugal

³ Nuffield Department of Orthopaedics, Rheumatology and Musculoskeletal Sciences, Botnar Research Centre, University of Oxford, Oxford, UK

⁴ Institute of Organic Chemistry and Biochemistry, Czech Academy of Sciences, Prague, Czech Republic

⁵ Patrick G Johnston Centre for Cancer Research, Queen's University, Belfast, UK

*Corresponding author. Tel: +44 028 9097 2700; E-mail: c.adrain@qub.ac.uk

**Corresponding author. Tel: +351 21 446 9322; E-mail: domingp@itqb.unl.pt

[†]These authors contributed equally to this work as senior authors

[‡]Present address: Center for Genomics and Systems Biology, New York University Abu Dhabi, Abu Dhabi, United Arab Emirates

complex, with nine subunits in mammals (Wideman, 2015). The EMC was initially described in yeast in a high throughput genetic screen for genes required for protein folding (Jonikas *et al*, 2009) and its mammalian counterpart was later identified as part of the interaction network of the ER-associated protein degradation machinery (Christianson *et al*, 2011).

The EMC was subsequently shown to serve as an insertase for specific polytopic membrane proteins that contain a signal anchor sequence (SAS), including a subset of G-protein coupled receptors (GPCR; Chitwood *et al*, 2018). A variety of experiments suggested that the EMC coordinates the insertion of the first TMD of the GPCRs, after which subsequent TMD insertions are EMC-independent and require the Sec61 translocon, via a “handing-off” mechanism that remains to be fully elucidated (Chitwood *et al*, 2018).

The structure of both the human and yeast EMC have recently been determined using cryo-electron microscopy (cryo-EM) (Bai *et al*, 2020; Miller-Vedam *et al*, 2020; O'Donnell *et al*, 2020; Pleiner *et al*, 2020) and a model has been proposed for EMC-mediated co- and post-translational insertion of client proteins (Pleiner *et al*, 2020). According to this model, a captured client protein is directed towards the membrane by the flexible cytosolic loop of EMC3, the insertase subunit of EMC; the EMC then presumably reduces the energetic cost of insertion by inducing a local thinning of the membrane and by arranging polar and positively charged residues within the bilayer. The client would then dissociate from EMC3, encountering EMC1's β propellers, which could act as a scaffold for co-factor recruitment (Bai *et al*, 2020; Pleiner *et al*, 2020).

The requirement for the EMC in the biogenesis of some TA proteins and the first TMD of some polytopic membrane proteins containing a SAS has been dissected *in vitro*, leading to a rationalisation of how EMC can act mechanistically. However, the EMC has also been shown to be required for the biogenesis of multi-pass membrane proteins enriched with “challenging” TMDs (Shurtleff *et al*, 2018). Indeed, the majority of proteins found to date to be affected by loss of EMC are neither TA nor SAS-containing membrane proteins, suggesting that much remains to be understood about EMC specificity for its client proteins (Shurtleff *et al*, 2018; Tian *et al*, 2019). These include the ABC transporter Yor1 in yeast (Louie *et al*, 2012; Lakshminarayan *et al*, 2020), acetylcholine receptor in *C. elegans* (Richard *et al*, 2013), rhodopsins (Taylor *et al*, 2005; Satoh *et al*, 2015; Hiramatsu *et al*, 2019; Xiong *et al*, 2020), the transient receptor potential (TRP) channel in *Drosophila* (Satoh *et al*, 2015), ABCA1 in mice (Tang *et al*, 2017) and mutant connexin32 (Coelho *et al*, 2019). Furthermore, EMC loss of function has also been associated with defects in phospholipid trafficking (Lahiri *et al*, 2014; Janer *et al*, 2016), cholesterol homeostasis (Volkmar *et al*, 2019), autophagosome formation (Li *et al*, 2013; Shen *et al*, 2016), viral pathogenesis (Bagchi *et al*, 2016, 2020; Savidis *et al*, 2016; Barrows *et al*, 2019; Lin *et al*, 2019), neurological defects (Harel *et al*, 2016) and male fertility (Zhou *et al*, 2018). Although this diversity in phenotypes is still an area of investigation, several of these examples impact unrelated membrane proteins with multiple TMDs (Chitwood & Hegde, 2019; Volkmar & Christianson, 2020) and many of these candidate EMC clients are neither TA nor SAS-containing proteins. An alternative possibility to EMC acting as an insertase for a broader range of TMD protein topologies is that some of these proteins may be “indirect” or “secondary clients” of the

EMC, for example, proteins whose biogenesis or stability depends on a direct EMC client protein.

In this study, we interrogated the *Drosophila* proteome in an effort to bioinformatically identify TA proteins that could have a dependency on the EMC for their biogenesis. Using a *Drosophila* larval eye imaginal disc assay, we identified two EMC clients: fan (farinelli), which controls sperm individualisation (Ma *et al*, 2010) and Xport-A (exit protein of rhodopsin and TRP-A) (Rosenbaum *et al*, 2011; Chen *et al*, 2015b), an essential chaperone for the biogenesis of both Rhodopsin-1 (Rh1) and the TRP (Transient Receptor Potential) channel, and their targeting to the rhabdomere, the light sensitive compartment of the photoreceptors. Interestingly, the biogenesis of Rh1 and TRP has been shown to be deficient in EMC mutant clones (Satoh *et al*, 2015; Hiramatsu *et al*, 2019; Xiong *et al*, 2020). We generated a mutant of Xport-A (Xport-A4L) whose biogenesis proceeds independently of the EMC. Xport-A4L is able to rescue the expression of Rh1 and TRP in EMC mutant tissue, suggesting that the latter proteins are not direct clients of the EMC but rather, depend on EMC indirectly via Xport-A. Overall, our results suggest that EMC is required for sperm and photoreceptor differentiation in *Drosophila*, due to EMC's role in the biogenesis of fan and Xport-A, respectively. Crucially, our data establish that EMC impacts the biogenesis of some multi-pass membrane proteins indirectly, by governing insertion of the cofactors they require for assembly and deployment. This paradigm expands the potential governance of the EMC to a greater portion of the membrane proteome.

Results

EMC is required for the biogenesis of a subset of tail-anchored (TA) proteins

The EMC has been shown to function as an insertase for TA proteins with TMDs of moderate to low hydrophobicity (Guna *et al*, 2018), but the identities of its clients have not been fully determined. To ascertain the range of EMC-dependent TA proteins, we began by screening the *Drosophila melanogaster* proteome for all possible TA proteins. TA proteins are defined by their cytosolic N-terminal domain that is anchored to the lipid bilayer by a single hydrophobic TMD proximal to the C-terminus (Borgese *et al*, 2003). We bioinformatically interrogated the proteome using prediction algorithms for: signal peptide, TMD and topology (Käll *et al*, 2005) as well as subcellular localisation (Almagro Armenteros *et al*, 2017) (Fig 1A). This analysis yielded a total of 254 candidate TA proteins in the *Drosophila* proteome, with predicted membrane localisations (Figs 1A and EV1B, Dataset EV1). We subsequently characterised the distribution of different biophysical features such as TMD length, TMD hydrophobicity, tail length and charge (Fig EV1C–F). These analyses show that within the list of predicted TA proteins, those that are ER-localised tend to have higher TMD hydrophobicity and length than their mitochondrial and peroxisomal counterparts (Fig EV1C–F), which is consistent with published predictions for both human (Costello *et al*, 2017) and *Arabidopsis* (Kriechbaumer *et al*, 2009) proteomes.

The TMDs of most predicted TA proteins (~67%) exhibited low hydrophobicity (Guna *et al*, 2018) (hydrophobicity value below 22

in the Zhao & London hydrophobicity scale (Zhao & London, 2006)). This proportion was maintained in most sub-cellular localisations including the ER, but was altered in the Golgi apparatus (75% proteins with high hydrophobicity), the peroxisome and mitochondria (100% of proteins with low hydrophobicity).

Next, we selected 23 candidate TA proteins to test for EMC3 dependency by monitoring their expression in EMC3 mutant clones in *Drosophila* larval eye imaginal discs (Figs 1B, E–J, and EV1A). This model enables candidate TA protein expression levels in WT and adjacent EMC3 mutant territories to be compared side-by-side,

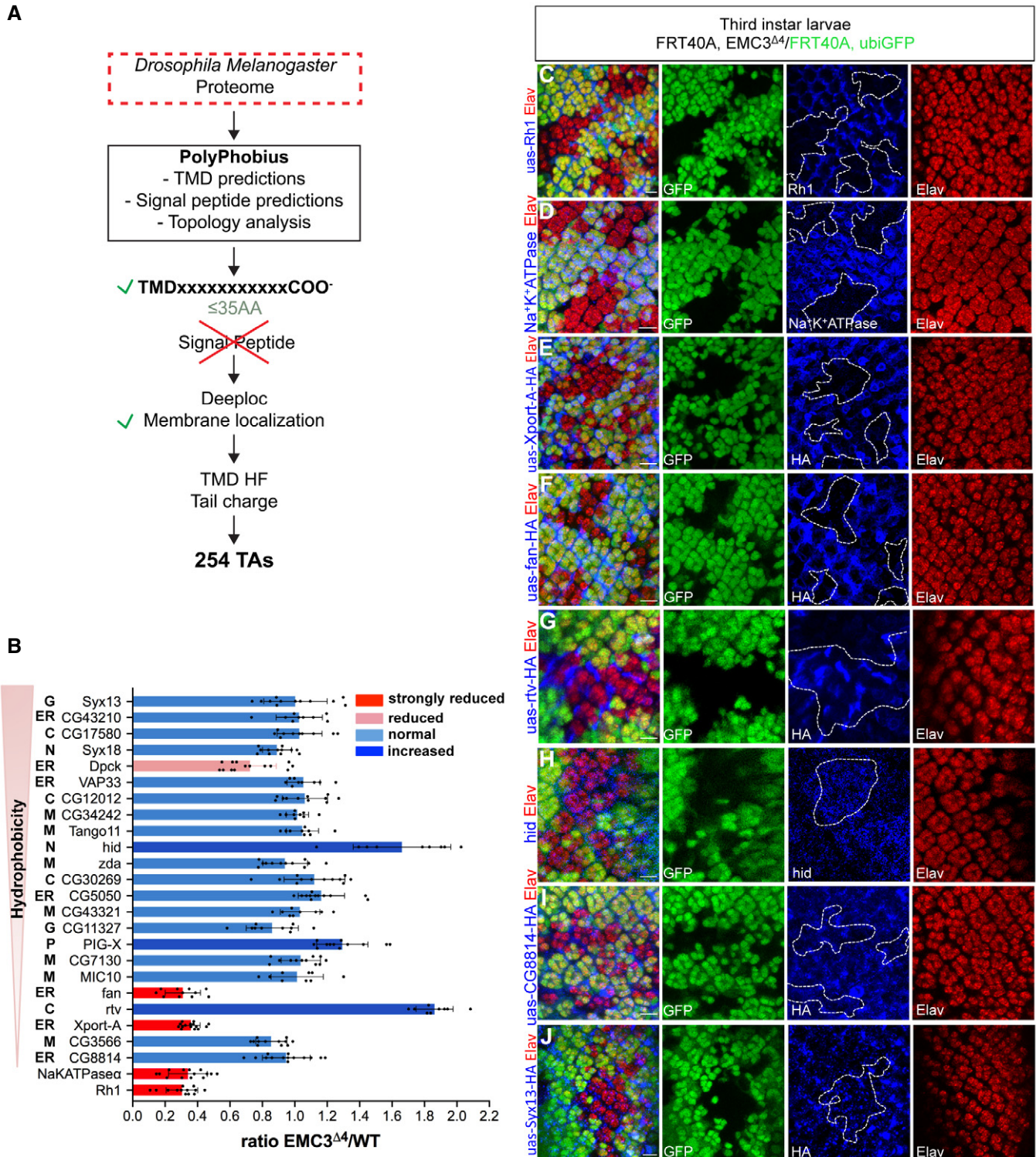


Figure 1.

Figure 1. EMC is required for the biogenesis of a subset of TA proteins.

- A The *Drosophila* proteome was screened to identify TA proteins using the PolyPhobius (Käll *et al*, 2005) algorithm within the TOPCONS (Tsirigos *et al*, 2015) web server. Proteins with a single TMD within 35 AAs or less upstream of the C terminus and lacking a signal peptide or mitochondrial targeting peptide were selected for further interrogation. The DeepLoc (Almagro Armenteros *et al*, 2017) predictor of protein sub-cellular localisation was used to eliminate soluble proteins from the list. These procedures yielded 254 proteins, which were scored for their tail charge and hydrophobicity using the “transmembrane tendency” score of Zhao & London (Zhao & London, 2006).
- B A subset of the predicted TA proteins was screened by overexpression in *Drosophila* larval eye imaginal discs containing clones of a previously isolated EMC3 mutant allele, EMC3^{A4} (Satoh *et al*, 2015). TA protein predicted membrane localisation is shown to the left: G (Golgi apparatus), ER (endoplasmic reticulum), C (cytoplasmic membrane), N (nucleus), M (mitochondria) and P (peroxisome). The ratio of fluorescence intensity for the tested TA proteins in EMC3 homozygous mutant cells over WT cells (EMC3^{A4}/WT) was measured and plotted. Proteins were classified into four groups according to the ratio measured: strongly reduced (ratio < 0.5; bars in red), reduced (ratio 0.5–0.8; bar in pink), normal (ratio 0.8–1.2; bars in blue) and increased (ratio > 1.2; bars in dark blue). For quantification, at least three mutant patches were quantified per eye imaginal disc, and at least three eye imaginal discs derived from distinct flies were used (*N* = 3). Error bars correspond to standard deviation (SD).
- C–J All panels show *Drosophila* third instar larval eye imaginal discs with eyeless-Flippase-induced clones of cells homozygous for EMC3^{A4} (Satoh *et al*, 2015), labelled by the absence of ubiGFP (green). The red channel shows ELAV, which labels the nuclei of photoreceptor cells. All UAS constructs were expressed under the control of GMR-GAL4. (C) Expression of UAS-Rh1 (4C5, in blue) and (D) Na⁺K⁺ATPase (A5-C, in blue) is strongly reduced in EMC3^{A4} homozygous mutant cells. (E) Expression of UAS-Xport-A-HA (anti-HA, in blue) and (F) UAS-fan-HA (anti-HA, in blue) is strongly reduced in EMC3^{A4} homozygous mutant cells. (G) Expression of UAS-rtv-HA (anti-HA, in blue) and (H) hid (anti-hid, in blue) is increased in EMC3^{A4} homozygous mutant cells. (I and J) Normal expression of two TA proteins in EMC3^{A4} homozygous mutant cells. (I) UAS-CG8814-HA (anti-HA, in blue) is a TA protein containing a TMD of low hydrophobicity (J) UAS-Syx13-HA is a TA protein with high hydrophobicity TMD. Scale bars represent 10 μm.

Source data are available online for this figure.

within the same tissue. Of the 23 proteins tested, ~87% had low predicted TMD hydrophobicity, were from within all predicted sub-cellular membrane localisations and had similar distribution of localisation to the overall pool of predicted TA proteins (Fig EV1A and B, Appendix Table S1). Candidate TA proteins were overexpressed under the control of GMR-GAL4 in larval eye imaginal discs containing EMC3 mutant (EMC3^{A4} (Satoh *et al*, 2015)) clones. EMC3 is considered a “core” subunit of the complex, with mutations in EMC3 and other core subunits (EMC1, 2, 5 and 6) causing significant impairment of EMC functionality (Guna *et al*, 2018; Volkmar *et al*, 2019; Volkmar & Christianson, 2020). Candidate TA protein expression was assayed by immunofluorescence using antibodies raised against the respective proteins or, when no suitable antibodies existed, against an appended HA (Hemagglutinin) tag. Rh1 and the Na⁺K⁺ATPase α subunit were also evaluated (Fig 1C and D), as their expression has been reported previously to be EMC dependent (Satoh *et al*, 2015; Hiramatsu *et al*, 2019; Xiong *et al*, 2020).

We evaluated TA candidate expression by determining the ratio of fluorescence intensity between the signal associated with the candidate TA protein in EMC3 mutant clones versus non-mutant (WT) clones (EMC3^{A4}/WT) (Fig 1B). TA candidate expression was classified into four groups according to the EMC3^{A4}/WT fluorescence intensity ratio: strongly reduced (ratio < 0.5, bars in red), reduced (ratio 0.5–0.8, bar in pink), normal (ratio 0.8–1.2, bars in blue), and increased (ratio > 1.2, bars in dark blue). Rh1 (Fig 1C) and the Na⁺K⁺ATPase α subunit (Fig 1D) exhibited strongly reduced expression in EMC3^{A4} mutant clones, consistent with previously published results in the adult/pupal eye (Satoh *et al*, 2015; Hiramatsu *et al*, 2019; Xiong *et al*, 2020). Expression of Dpck was reduced in EMC3^{A4} mutant clones while rtv (Fig 1G), hid (Fig 1H) and PIG-X showed increased expression. Notably, two TA candidates, Xport-A (Fig 1E) and fan (Fig 1F), showed strongly reduced expression in EMC3^{A4} mutant clones compared to WT. Both proteins are predicted to localise to the ER membrane and contain TMDs of low hydrophobicity.

Of the 23 TA proteins tested, 17 exhibited normal ratios of expression, demonstrating that the GMR-GAL4 driven transcription

of the candidate proteins is not affected by the loss of EMC function. Examples of TA proteins with TMDs of low hydrophobicity (CG8814 – Fig 1I) and high hydrophobicity (Syx13 – Fig 1J) showing normal EMC3^{A4}/WT fluorescence intensity ratios could also be found.

EMC is required for sperm differentiation in *Drosophila*

Our screen identified the predicted TA protein fan, whose expression was defective in EMC3^{A4} homozygous mutant clones (Fig 1F). As fan reportedly plays an important role in sperm individualisation and male fertility (Ma *et al*, 2010) (Fig EV2A), we asked whether the EMC was also required for male fertility in *Drosophila*. We selected RNAi lines targeting different EMC subunits (EMC1, EMC3, EMC4, EMC5, EMC6, EMC7, EMC8/9) and mated adult males in which individual EMC subunits were knocked down, with wild-type virgin females (Fig EV2B and C). We counted the mean number of progeny obtained from these crosses and observed a statistically significant reduction for all RNAi lines of EMC5 and EMC6, and for one RNAi line of EMC1 (Fig EV2B). We analysed sperm vesicle size and observed that, in accordance with the reduced male fertility, all EMC5 and EMC6 RNAi lines tested exhibited a statistically significant reduction in sperm vesicles (Fig EV2D), which correlates with a reduction in sperm production (Ma *et al*, 2010; Chen *et al*, 2015a). Furthermore, the seminal vesicles of flies expressing EMC5_2 RNAi line appeared devoid of mature sperm, as the needle shaped nuclei of mature sperm were absent (Fig EV2E). Finally, we tried to address the cause of male fertility in an EMC5 RNAi line, observing that while staining with an antibody against active Caspase-3 was present in multiple cystic bulges (cb) in wild-type testis, this staining was deficient in EMC5 RNAi testis (Fig EV2F), demonstrating sperm differentiation defects, as previously shown (Arama *et al*, 2003).

EMC3 is required for the expression of Xport-A, but not Xport-A4L

Although the specificity of EMC for its clients remains to be fully delineated, the EMC exhibits a preference for TA proteins with low

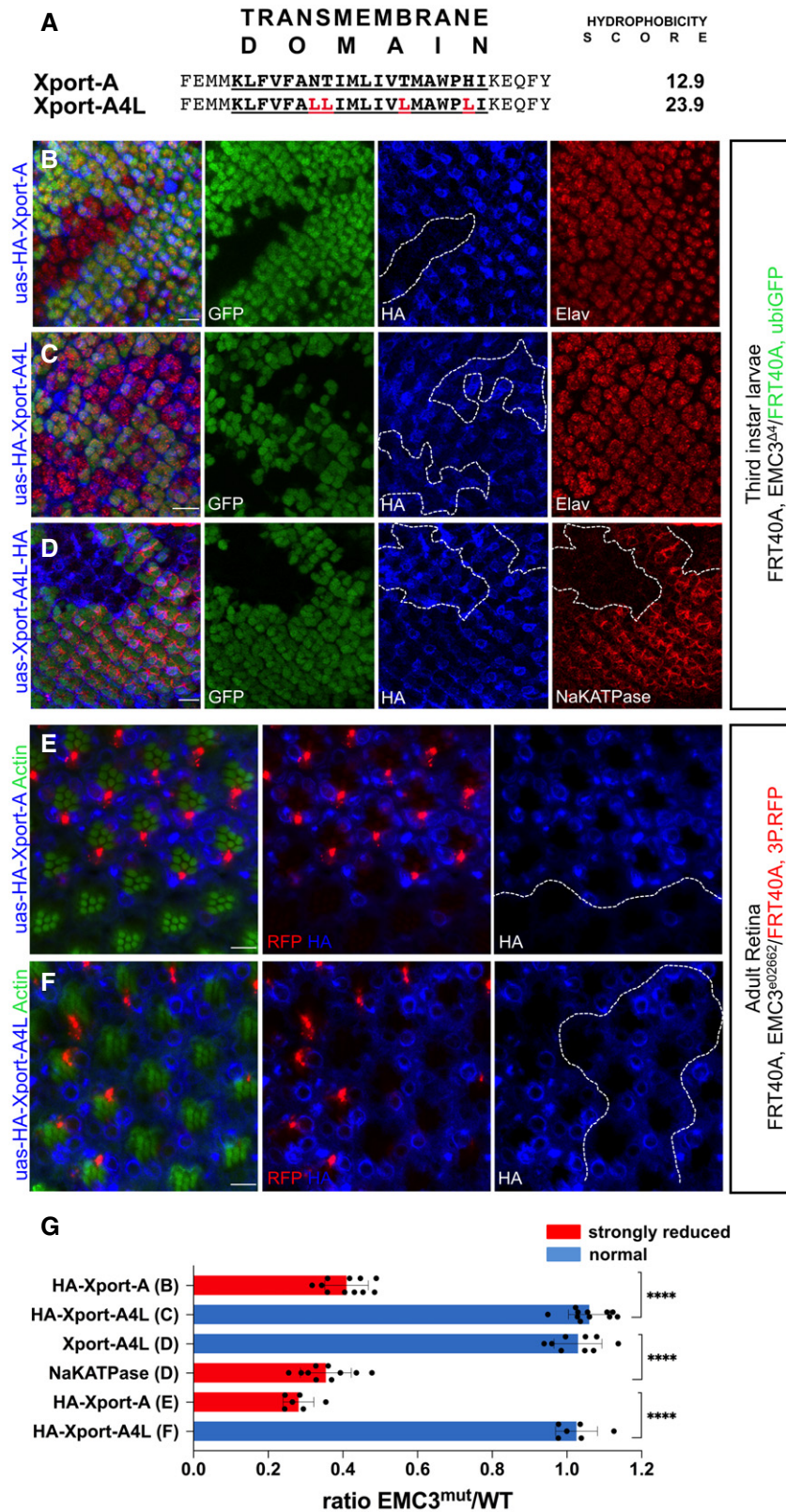


Figure 2.

Figure 2. EMC3 is required for the expression of Xport-A, but not Xport-A4L

- A The TMD of Xport-A was identified using TOPCONS (Tsirigos *et al*, 2015) and is in bold/underlined, together with the immediate flanking residues. Red residues indicate mutations made in the Xport-A TMD to increase its hydrophobicity, creating the Xport-A4L mutant. To the right of each sequence is the “transmembrane tendency” score, calculated according to Zhao & London (2006).
- B–D Immunostaining of third instar larval eye imaginal discs with eyeless-Flippase-induced clones of cells homozygous for EMC3^{A4}, labelled by the absence of ubiGFP (green) shows reduced expression of (B) UAS-HA-Xport-A (anti-HA, in blue) but normal expression of (C) UAS-HA-Xport-A4L (anti-HA, in blue) or (D) UAS-Xport-A4L-HA (anti-HA, in blue) in EMC3 mutant homozygous cells. ELAV (red in B and C) marks photoreceptor cells and Na⁺K⁺ATPase (red in D) acts as a positive control for the presence of EMC3^{A4} homozygous mutant clones. The UAS constructs were expressed under the control of GMR-GAL4. Scale bars represent 10 μm.
- E, F Immunostaining of mosaic adult retina with eyeless-Flippase-induced clones of cells homozygous for EMC3^{e02662}, labelled by the absence of RFP (red), show loss of (E) UAS-HA-Xport-A (anti-HA, in blue) in EMC3 mutant homozygous cells. (F) Expression of UAS-HA-Xport-A4L (anti-HA, in blue) is normal in EMC3^{e02662} homozygous mutant clones. The rhabdomeres are stained for actin (Phalloidin, in green). Scale bars represent 10 μm.
- G The ratio of fluorescence intensity in EMC3 homozygous mutant cells over that of WT cells (EMC3^{mut}/WT) was measured and plotted. Proteins were classified into two groups according to the ratio measured: strongly reduced (ratio < 0.5; bars in red) and normal (ratio 0.8–1.2; bars in blue). For quantification, at least three mutant patches were quantified per eye imaginal disc, and at least two mutant patches were quantified per adult retina. At least three eye imaginal discs or adult retina derived from distinct flies were used (N = 3). Error bars correspond to SD. Significance was determined by Welch's t-test: ****P ≤ 0.0001.

Source data are available online for this figure.

TMD hydrophobicity and/or containing polar/charged amino acid residues (Guna *et al*, 2018; Tian *et al*, 2019; Volkmar *et al*, 2019). As the Xport-A TMD has a reduced hydrophobicity due to the presence of one polar and multiple charged residues, an Xport-A TMD with increased hydrophobicity would be expected to relieve its EMC dependency. To that end, we performed site-directed mutagenesis on the Xport-A TMD to substitute the four most hydrophilic amino acids with leucine, creating the mutant Xport-A4L (Fig 2A). As hypothesised, whereas WT HA-Xport-A was dependent on the EMC (Fig 2B and G), expression of HA-Xport-A4L (Fig 2C and G) or Xport-A4L-HA (Fig 2D and G) no longer required EMC3 in larval eye imaginal discs. Importantly, the levels of the Na⁺K⁺ATPase α control protein remained defective in EMC3 mutant clones (Fig 2D and G), confirming the presence of “bona fide” EMC3 mutant clones in the eye disc and demonstrating the specificity of the rescue effect of the Xport-A4L mutant for Xport-A targets, but not for EMC clients in general. A similar impact of the Xport-A4L mutant was observed in experiments carried out in adult retinas (Figs 2E–G and EV3A). Altogether, these results indicate that increasing the hydrophobicity of the Xport-A TMD renders its expression independent of the EMC and that tagging Xport-A and Xport-A4L at either the N- or C-terminus yields identical results.

EMC is required for the biogenesis of Xport-A in mammalian cells

We next sought to confirm the dependence of Xport-A biogenesis on the EMC using an assay independent of *Drosophila*. We cloned the TMDs of Xport-A, Xport-A4L and the validated EMC client squalene synthase (SQS) (Guna *et al*, 2018; Volkmar *et al*, 2019), individually into the dual fluorescent reporter GFP-P2A-RFP (Fig 3A). When translated in mammalian cells, this mRNA will generate two different products due to peptide bond skipping induced by the P2A site: GFP and RFP-SQS, RFP-Xport-A or RFP-Xport-A4L. A stable GFP serves as a reporter for translation of the construct that enables quantitative read-out for protein stability through fluorescence ratios (Chitwood *et al*, 2018). When the RFP:GFP ratio is reduced, it reflects post-translational degradation of the RFP-client protein fusion, presumably due to a failure to integrate into the ER membrane. In human U2OS cells lacking the core subunit EMC5 (Δ EMC5) (Guna *et al*, 2018; Volkmar *et al*, 2019) (Fig EV3B), transiently expressed GFP-P2A-RFP-Xport-A exhibited a reduced RFP:

GFP ratio when compared to WT U2OS cells (Fig 3C). Induced expression of EMC5 in Δ EMC5 cells restored the EMC and resulted in a RFP:GFP ratio that was comparable to WT cells (Fig 3C). Similar results were obtained from cells lacking the core subunit EMC6 (Δ EMC6, Fig 3F). In fact, Xport-A behaved comparably to SQS (Fig 3B and E), a TA protein involved in cholesterol homeostasis whose biogenesis has been established as EMC-dependent (Guna *et al*, 2018; Volkmar *et al*, 2019). Importantly, there was no difference in the measured RFP:GFP ratios following expression of GFP-P2A-RFP-Xport-A4L in Δ EMC5 or Δ EMC6 cells, when compared to either WT or EMC rescue cell lines (Fig 3D and G). These results indicate that the EMC is important for post-translational stability of Xport-A and that this effect relies on the low hydrophobicity of its TMD.

EMC6 is required for membrane insertion of Xport-A TMD

Xport-A is a TA protein and its TMD must be inserted post-translationally into the ER membrane. To monitor insertion efficiency in the ER membrane, we cloned the TMDs from Sec61 β , SQS, and Xport-A into a common cassette containing a C-terminal opsin tag (Fig 4A and B). The opsin tag, if exposed to the ER lumen, is able to accept N-linked oligosaccharides, serving as an indicator of successful TMD insertion into the membrane (Brambillasca *et al*, 2005). The SQS TMD reporter is glycosylated in WT cells, but fails to be glycosylated in Δ EMC6 cells (Fig 4C and E), as previously reported (Guna *et al*, 2018; Volkmar *et al*, 2019). In contrast, the majority of the Sec61 β reporter remains glycosylated in Δ EMC6 cells (Fig 4C and E), consistent with its EMC-independent insertion pathway (Guna *et al*, 2018). As predicted by our *Drosophila* results (Figs 1 and 2), the Xport-A TMD reporter is glycosylated in WT cells, but does not undergo glycosylation in Δ EMC6 cells (Fig 4D and E), behaving similarly to HA-SQS-opsin (Fig 4C).

Next, we sequentially mutagenised the TMD of Xport-A to substitute the four most hydrophilic AAs with leucine (Fig 4B). By progressively increasing the hydrophobicity of Xport-A TMD, we attempted to identify a TMD hydrophobicity threshold for EMC recognition. A single point mutant of the Xport-A TMD (Xport-A1L) retained its dependence on the EMC for membrane insertion (Fig 4F and G), but subsequent mutations (Xport-A2L, -A3L) were increasingly glycosylated in Δ EMC6 cells (Fig 4F and G). With four leucine mutations in the Xport-A TMD (Xport-A4L), insertion became

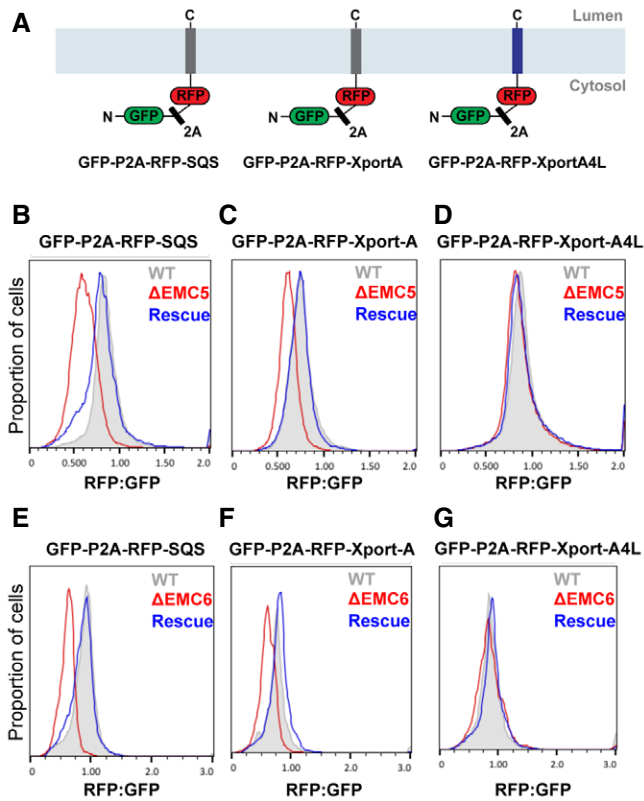


Figure 3. EMC is required for the biogenesis of Xport-A in mammalian cells.

- A** Schematic representation of the reporter constructs used for analysis of protein biogenesis by flow cytometry. All constructs contain an N-terminal GFP and a C-terminal RFP, separated by a viral 2A peptide that mediates peptide bond skipping. Changes in the stability of SQS, Xport-A and Xport-A4L fused to RFP change the RFP:GFP fluorescence ratio.
- B–D** Histograms of flow cytometry data monitoring the fluorescence protein ratio in the indicated U2OS cell lines for each construct. “EMC5KO + EV” indicates a knockout of EMC5 stably harbouring empty vector, while “EMC5KO + EMC5” indicates EMC5KO cells rescued by inducible re-expression of a stably integrated EMC5.
- E–G** Histograms of flow cytometry data monitoring the fluorescence protein ratio in the indicated U2OS cell lines for each construct. “EMC6KO + EV” indicates a knockout of EMC6 stably harbouring empty vector, while “EMC6KO + EMC6” indicates EMC6KO cells rescued by re-expression of a stably integrated EMC6.

entirely EMC independent, as indicated by the glycosylation pattern equivalent to what is observed in WT cells (Fig 4D). This finding supports the existence of a TMD “hydrophobicity threshold” that directs clients to insert in the ER membrane via the EMC.

Expression of Xport-A4L can rescue Rh1 and TRP biogenesis defects in EMC3 mutant clones

Xport-A serves as an essential chaperone during the biogenesis and maturation of both Rh1 and TRP; proteins that are essential for light sensing within the rhabdomere (Rosenbaum *et al*, 2011; Chen *et al*, 2015b). The protein levels of both Rh1 and TRP are significantly reduced in Xport-A loss of function mutations (Rosenbaum *et al*,

2011; Chen *et al*, 2015b), as well as in EMC mutations (Satoh *et al*, 2015; Hiramatsu *et al*, 2019; Xiong *et al*, 2020). Our demonstration that Xport-A is a client protein of the EMC, raised the possibility that loss of TRP and Rh1 observed in EMC mutants could instead be attributable to failed membrane insertion and biogenesis of Xport-A. To test this hypothesis, we compared the capacity of Xport-A and Xport-A4L to rescue expression of Rh1 and TRP in EMC mutant clones. While Xport-A overexpression in EMC3 mutant clones was unable to rescue Rh1 (Fig 5A and E), we did find that Xport-A4L expression was sufficient to significantly restore Rh1 protein levels in EMC3^{Δ4} clones (Fig 5B and E). Similarly, Xport-A overexpression in the adult retina in cells homozygous for a hypomorphic mutation of EMC3 (EMC3^{e02662}) was unable to rescue TRP expression (Fig 5C and E). On the other hand, overexpression of Xport-A4L was sufficient to rescue endogenous expression of TRP in EMC3^{e02662} clones (Fig 5D and E). Additionally, we find that another Xport-A mutant, Xport-A2L, significantly rescued Rh1 expression in EMC mutant clones (Fig EV4A–C). Together, these data suggest that Rh1 and TRP biogenesis and maturation are not directly dependent on the EMC, but rather appear to be indirectly dependent on it, via the membrane insertion of Xport-A.

Glycosylated Rh1 TMD1-5 accumulates in Xport-A and EMC6^{N10} homozygous mutants

A previous study dissected the requirement of the EMC in the biogenesis of a series of Rh1 truncation mutants, identifying that EMC is required for the synthesis of Rh1 TMD1-5, but not TMD1 nor TMD1-3 (Hiramatsu *et al*, 2019). This indicates that a key determinant of Rh1’s biogenesis dependency on the EMC is contained within TMDs 4 or -5. As our data show that Rh1 biogenesis is influenced indirectly by EMC, via the EMC client Xport-A, this predicts that this key feature encoded within TMDs 4 or -5 should also be crucial for Rh1’s biogenesis dependency on Xport-A.

The immature/ER form of endogenous Rh1 (Fig 6A) initially acquires Endoglycosidase H (Endo-H)-sensitive glycans, after which its progression in the secretory pathway results in its maturation to a lower molecular weight, fully de-glycosylated species (Rosenbaum *et al*, 2014). To examine the impact of Xport-A on the biogenesis of these truncations, we expressed Rh1 TMD1, TMD1-3 and TMD1-5 in Xport-A heterozygous versus homozygous mutant fly eyes (Fig 6) and monitored the sensitivity of these proteins to Endo-H and PNGase. For TMD1 (Fig 6B and E) and TMD1-3 (Fig 6C and F), there was no difference in the expression of the V5-tagged constructs between Xport-A mutant heterozygotes or homozygotes, similar to the results observed in EMC-deficient clones (Hiramatsu *et al*, 2019). These truncations comprise a single PNGase-sensitive band, indicating the presence of glycans, presumably due to glycosylation at N20 as was previously reported for Rh1 (O’Tousa, 1992; Katano-saka *et al*, 1998; Webel *et al*, 2000). However, for the TMD1-5 truncation (Fig 6D and G), we observed the accumulation of two distinct Endo-H-sensitive bands: an upper band that was highly enriched in Xport-A homozygous mutants, and a lower band that was detected in both Xport-A mutant heterozygotes and homozygotes (Fig 6G). As both bands were Endo-H-sensitive, our interpretation is that Rh1 TMD1-5 is normally glycosylated at N20 but acquires an additional Endo-H sensitive glycan. Given that Rh1 contains a second glycosylation site at N196, we mutated this residue to isoleucine (N196I)

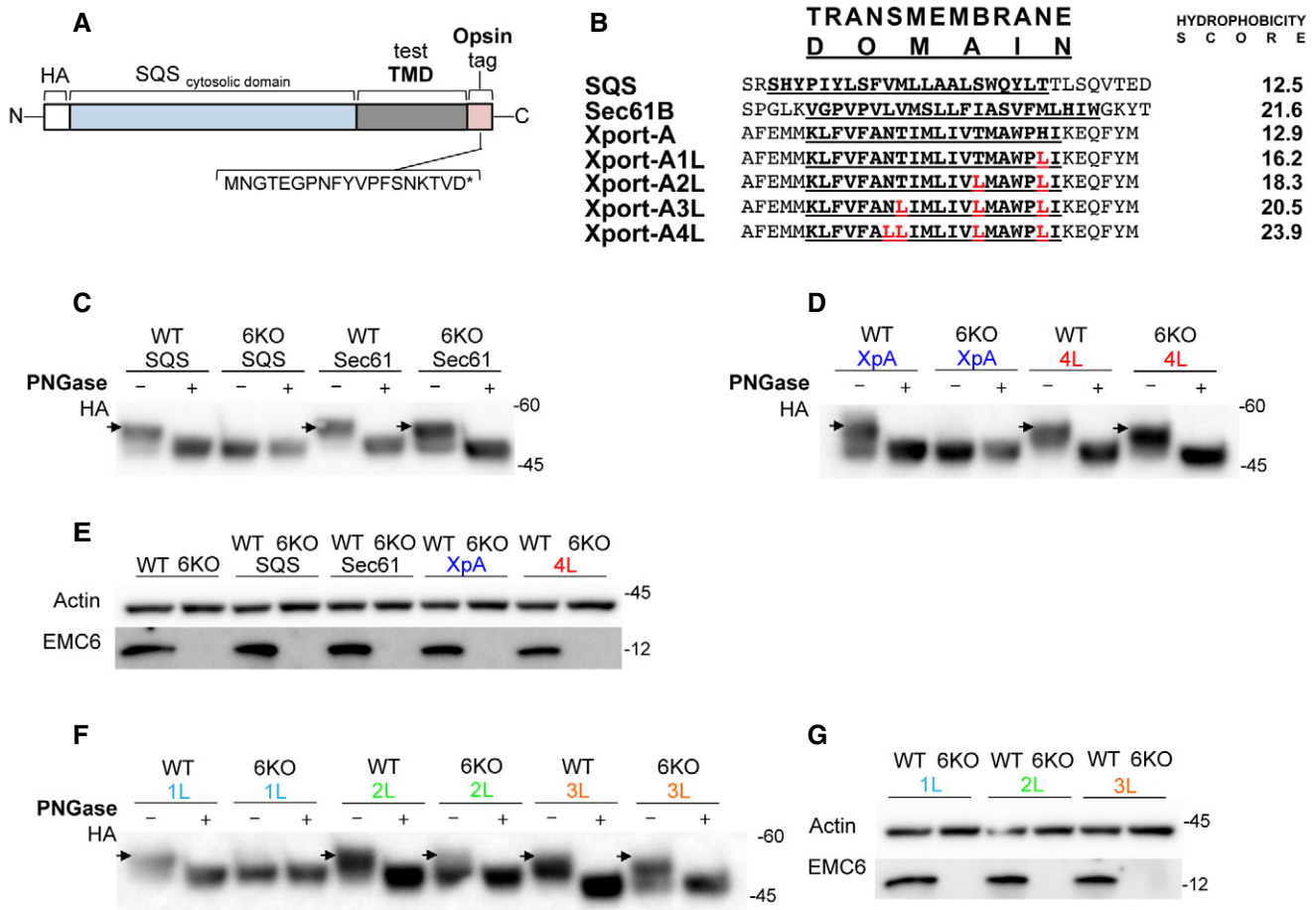


Figure 4. EMC6 is required for membrane insertion of Xport-A TMD.

- A** Schematic representation of the constructs used to monitor insertion efficiency in the ER membrane. All constructs contain a HA-tagged SQS cytosolic domain fused to a varying TMD sequence, which is C-terminally fused to an opsin tag (sequence indicated). Glycosylation of the C-terminal opsin tag acts as a readout for insertion into the ER.
- B** Sequences of the TMD regions used for cloning and the immediate flanking residues are represented. The regions defined as TMDs were determined using TOPCONS (Tsirigou *et al*, 2015) and are in bold/underlined. Red residues indicate mutations made in the Xport-A TMD to increase its hydrophobicity. To the right of each sequence is the “transmembrane tendency” score of Zhao & London (2006).
- C–G** Western-Blot of WT and EMC6KO (6KO) U2OS cell lines transiently transfected with the opsin-tagged constructs probed for HA. When indicated, denatured samples were treated with PNGase to confirm glycosylation. Glycosylated proteins shift upwards in the gel and are indicated by arrows (→). (E, G) Western-Blot of WT and EMC6KO (6KO) U2OS cell lines transiently transfected with the opsin-tagged constructs probed for Actin and EMC6.

Source data are available online for this figure.

and expressed this construct in Xport-A mutant heterozygous and homozygous flies. As shown in Fig EV5A, for Rh1 TMD1-5 N196L, we observed the accumulation of only one Endo-H-sensitive band in Xport-A heterozygous and homozygous mutants, instead of the two “glyco” bands observed in Xport-A homozygotes, when N196 is available for glycosylation (Fig 6G). From these results, we conclude that in Xport-A homozygous mutants, double glycosylated (N20 and N196) Rh1 TMD1-5 accumulates in the ER, and that, perhaps, the actual role of Xport-A is to somehow inhibit glycosylation at N196, which could otherwise be detrimental for the biogenesis of Rh1.

As our data support a model whereby Xport-A and not Rh1 is a client of the EMC, an important prediction is that Rh1 TMD1-5 should exhibit a similar glycosylation pattern in Xport-A and EMC-

deficient tissues. To test this, while avoiding the small eye phenotype associated with the complete deletion of EMC in the adult eye, we used the previously described mutant EMC6^{N10} (Xiong *et al*, 2020) in whole eye mutant clones (with FRT GMR-hidCL technique—Fig EV5B and C). As shown in Fig EV5B, EMC6^{N10} adult eyes have reduced levels of the EMC complex, as judged by the reduction in EMC3 expression and also have significantly depleted levels of endogenous Xport-A, as anticipated from our previous results. Moreover, as we observed with loss of Xport-A (Fig 6G), EMC6^{N10} mutant eyes have increased levels of the hyperglycosylated form of Rh1 TMD1-5 (Fig EV5C). Taken together, our results imply that Xport-A is required to ensure the proper folding of Rh1 and/or for the recognition and subsequent degradation of glycosylated (and presumably misfolded) Rh1 that would otherwise accumulate in the

ER. These data imply a novel role for Xport-A in acting at a key triage step for Rh1 biogenesis within the ER.

Discussion

Understanding the full scope of client proteins that depend on the EMC for biogenesis and maturation is yet to be fully appreciated. Here, we describe an approach to predict, screen, and validate candidate EMC client proteins, which we applied to the *Drosophila*

TA proteome. From a subset of TA candidate proteins with low predicted hydrophobicity scores, we identified fan and Xport-A as novel clients of the EMC. Taken together with previous studies that identified SQS, a key enzyme in sterol biogenesis (Guna *et al*, 2018; Volkmar *et al*, 2019) and ZFPL1, a zinc-finger containing protein required for efficient ER to Golgi transport/integrity of the *cis-Golgi* (Chiu *et al*, 2008; Tian *et al*, 2019), our observations emphasise the importance of the EMC as an insertase for a subset of TA proteins whose insertion is independent of the GET/TRC40-complex. Taken together with previous studies (Guna *et al*, 2018; Tian *et al*, 2019;

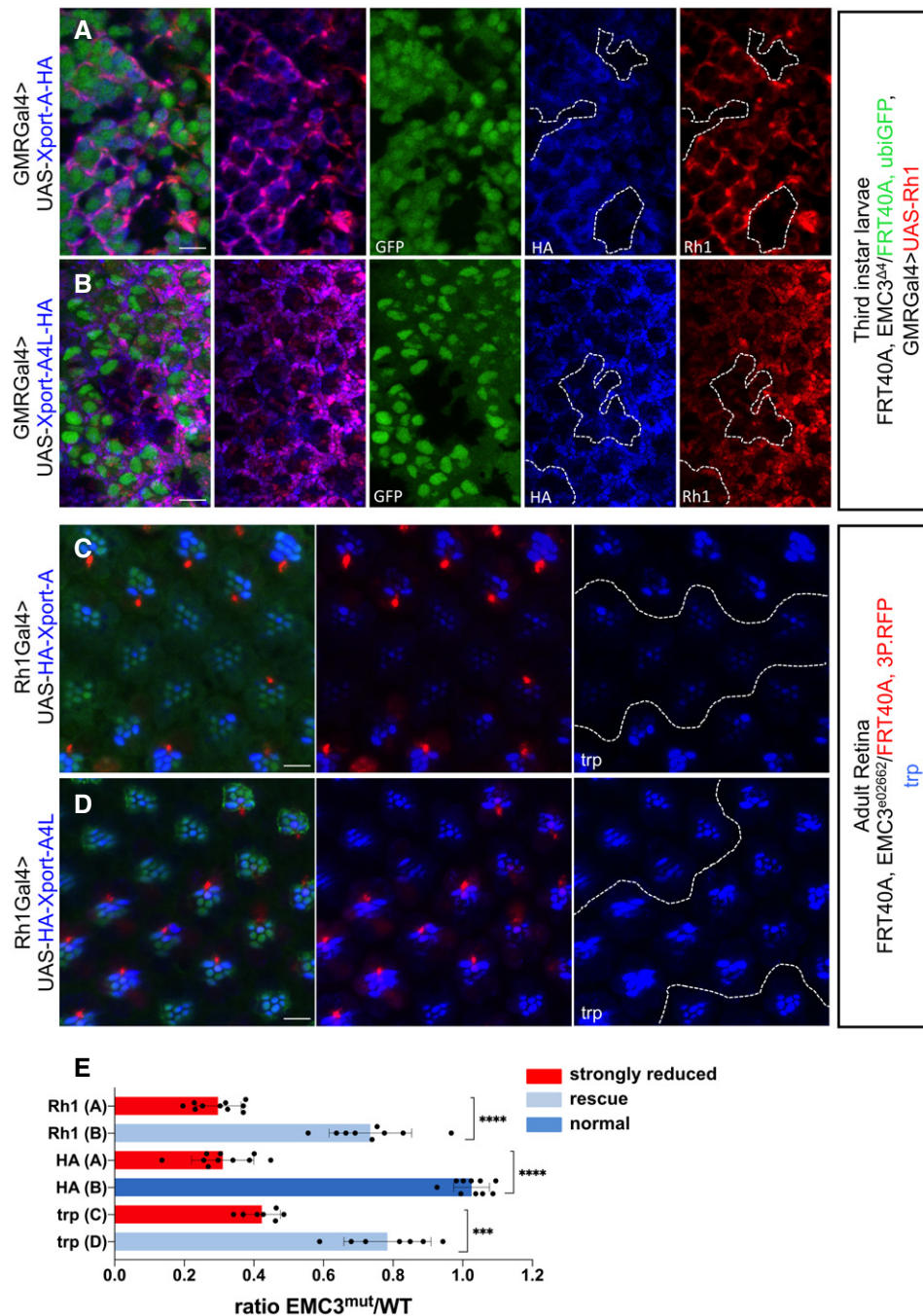


Figure 5.

Figure 5. Expression of Xport-A4L can rescue Rh1 and TRP biogenesis defects in EMC3 mutant clones.

- A, B Immunostaining of third instar larval eye imaginal discs with eyeless-Flippase-induced clones of cells homozygous for EMC3^{A4}, labelled by the absence of ubiGFP (green) show loss of (A) UAS-Xport-A-HA (anti-HA, in blue) and UAS-Rh1 (4C5, in red). (B) Expression of UAS-Xport-A4L (anti-HA, in blue) and UAS-Rh1 (4C5, in red) is observed in EMC3^{A4} homozygous cells. The UAS constructs were expressed under the control of GMR-GAL4. Scale bars represent 10 μ m.
- C, D Immunostaining of mosaic adult retinas with eyeless-Flippase-induced clones of cells homozygous for EMC3^{E02662}, labelled by the absence of RFP (red), show loss of (C) TRP (Mab83F6, in blue) when UAS-HA-Xport-A is expressed. (D) Expression of TRP (Mab83F6, in blue) is observed in EMC3^{E02662} homozygous cells, when HA-Xport-A4L is expressed. The rhabdomeres are stained for actin (Phalloidin, in green). The UAS constructs were expressed under the control of Rh1-GAL4. Scale bars represent 10 μ m.
- E The ratio of fluorescence intensity in EMC3 homozygous mutant cells over that of WT cells (EMC3^{mut}/WT) was measured and plotted. Proteins were classified into three groups according to the ratio measured: strongly reduced (ratio < 0.5; bars in red), rescue (ratio 0.5–0.8, bars in light blue) and normal (ratio 0.8–1.2; bar in dark blue). For quantification, at least three mutant patches were quantified per eye imaginal disc, and at least two mutant patches were quantified per adult retina. At least three eye imaginal discs or adult retina derived from distinct flies were used ($N = 3$). Error bars correspond to SD. Significance was determined by Welch's t -test: *** $P \leq 0.001$, **** $P \leq 0.0001$.

Source data are available online for this figure.

Volkmar *et al*, 2019), our data also demonstrate conservation of the EMC's ability to recognise TA proteins with reduced TMD hydrophobicity caused by the presence of charged/polar residues. Notably, the EMC appears to have additional levels of selectivity for TA client proteins. Even though our predictions identified multiple candidate proteins with reduced TMD hydrophobicity, only a small fraction of these were confirmed as clients in our genetic screen in *Drosophila*. Future studies will be required to dissect the precise basis whereby the presence, nature, and position of non-hydrophobic residues confers EMC dependency.

Fan is a member of the VAP (VAMP associated protein) family of proteins that bind OSBPs (Oxysterol binding proteins) and plays a role in sterol trafficking, including in the "individualisation complex", a cellular structure that promotes the membrane reorganisation process (sperm individualisation) that is crucial for the production of mature, functional sperm. Consistent with the role for fan in sperm individualisation, depletion of several independent EMC subunits in testis (particularly EMC5, EMC6) render male flies infertile, with individualisation defects similar to those reported for ablation of fan or OSBP family proteins (Ma *et al*, 2010). Our identification of Fan as an EMC client, further strengthens the connections between the EMC and sterol homeostasis, established by the identification of SQS and SOAT1 as EMC clients (Guna *et al*, 2018; Volkmar *et al*, 2019).

The identification of Xport-A as an endogenous EMC client raises some interesting questions. The Xport locus, consisting of the bicistronic operon separately encoding the Xport-A and Xport-B proteins, is required for the stable expression and localisation of Rh1 (a GPCR) and TRP (a calcium ion channel) to the rhabdomeres (Rosenbaum *et al*, 2011; Chen *et al*, 2015b). Loss of Xport proteins results in depletion of Rh1 and TRP, causing photoreceptor degeneration and visual impairment. Intriguingly, as highlighted above, several studies have reported the loss of Rh1, TRP, and accompanying photoreceptor degeneration in EMC-mutant flies (Satoh *et al*, 2015; Hiramatsu *et al*, 2019; Xiong *et al*, 2020). As polytopic membrane proteins, Rh1 and TRP could directly engage the EMC during their biogenesis. However, our identification of Xport-A as an EMC client suggested the possibility that EMC governance over Rh1 and TRP expression could be indirect. Such a model is supported by the results obtained with the Xport-A mutants engineered to be EMC-independent (Xport-A4L, Xport-A2L), which are sufficient to rescue expression of both Rh1 and TRP in mutant clones lacking functional EMC (Figs 5 and EV4). Moreover, in the heterologous setting of

mammalian cells where neither Rh1 nor TRP are expressed, Xport-A remains an EMC client with no collateral impact on its biogenesis. Conceptually, a model where "third party" proteins are lost as an indirect consequence of impaired biogenesis of a bona fide EMC client protein could help to explain the pleiotropic impact of loss on multiple classes of membrane proteins when EMC is ablated. While an attractive hypothesis, some important caveats could apply to the model above. First, Rh1 is a GPCR, a class of proteins that contain an N-terminal SAS which have recently been proposed to be direct EMC clients (Chitwood *et al*, 2018). Chitwood and colleagues showed that the EMC can mediate the insertion of the first TMD of some SAS-containing GPCRs, after which insertion proceeds co-translationally in a Sec61-translocon-dependent manner (Chitwood *et al*, 2018). However, this study did not investigate the requirement of EMC for *Drosophila* Rh1 membrane insertion. Moreover, expression levels of a Rh1 C-terminal truncation containing only the first TMD were uncompromised in EMC mutant *Drosophila* retinal cells (Hiramatsu *et al*, 2019). In fact, only a truncation containing the first 5 of the 7 Rh1 TMDs was expressed at lower levels in EMC mutant tissue (Hiramatsu *et al*, 2019). This study did, however, assess expression levels of Rh1 mutants by immunofluorescence, only, and did not investigate either Rh1 TMD membrane insertion or topogenesis.

Our studies suggest an interesting potential novel role for Xport-A, beyond its proposed role as a transport or targeting factor for Rh1 (Rosenbaum *et al*, 2011; Chen *et al*, 2015b). Through the use of Rh1 TMD truncations, we observed that the loss of Xport-A (Fig 6) or the EMC (Fig EV5B and C) result in the appearance of hyperglycosylated Rh1 TMD1-5, presumably via glycosylation of both N20 and N196. Notably, a previous study (Katanosaka *et al*, 1998) identified the N196 glycosylation site, which maps to the extracellular loop between TMDs 4 and 5 of Rh1. Although glycosylation at N196 has not been reported in WT or *ninaA* mutant flies (O'Tousa, 1992; Katanosaka *et al*, 1998; Weibel *et al*, 2000), this study showed N196 glycosylation with an *in vitro* translation system with mammalian microsomes (Katanosaka *et al*, 1998), i.e., a context that lacks Xport-A expression. Hence, it is tempting to speculate that Xport-A fulfils an important triage role in the ER during Rh1 biogenesis, by either directly or indirectly, inhibiting the glycosylation of Rh1 at N196, which could be essential for proper folding of Rh1. As onward trafficking from the ER is contingent on correct protein folding, a triage function of Xport-A would be predicted to impact on the subsequent trafficking aspects of Rh1, as previously reported for Xport-A (Rosenbaum *et al*, 2011; Chen *et al*, 2015b).

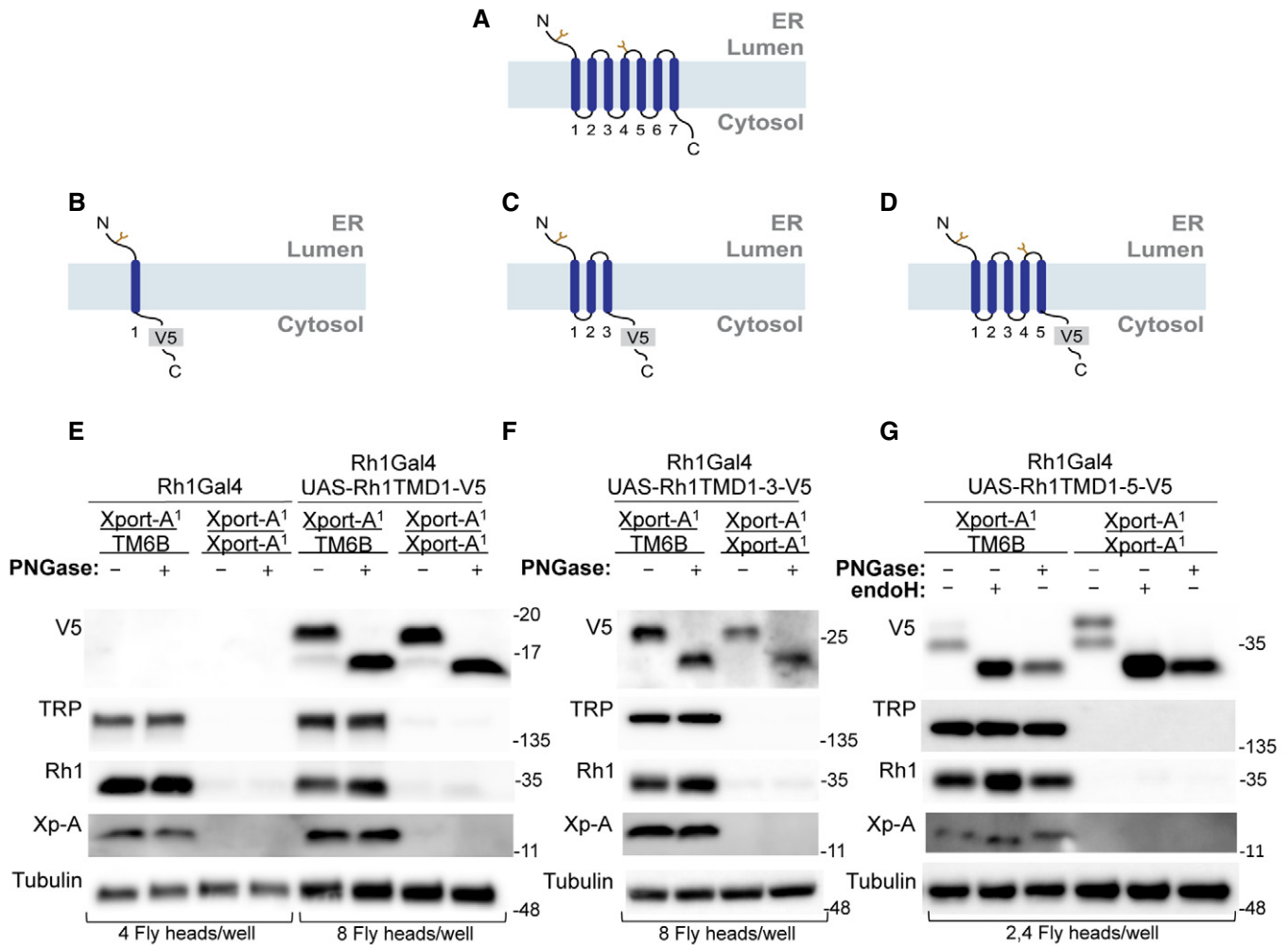


Figure 6. Glycosylated Rh1 TMD1-5 accumulates in Xport-A homozygous mutants.

A Schematic representation of endogenous Rh1. Predicted glycosylation sites (N20 and N196) are shown in yellow.

B–D Schematic representation of the Rh1 TMD1, TMD1-3 and TMD1-5 truncation constructs used to monitor glycosylation efficiency in Xport-A¹ mutants. Predicted glycosylation sites are shown in yellow.

E–G Western blot of fly heads labelled for V5, TRP, Rh1, Xport-A (Xp-A), and tubulin. (E) Immunoblot of fly heads expressing Rh1Gal4 (driver) (left) or Rh1 TMD1-V5 (right) in Xport-A heterozygous (Xport-A¹/TM6B) or homozygous mutant flies (Xport-A¹/Xport-A¹). Extracts were untreated (–) or treated (+) with PNGase F enzyme (lanes 2, 4, 6, and 8). For Rh1Gal4, four fly heads were loaded per well, while for Rh1 TMD1-V5, eight fly heads were loaded per well. (F) Immunoblot of fly heads expressing Rh1 TMD1-3-V5 in Xport-A heterozygous (Xport-A¹/TM6B) or homozygous mutant flies (Xport-A¹/Xport-A¹). Extracts were untreated (–) or treated (+) with PNGase F enzyme (lanes 2 and 4). Eight fly heads were loaded per lane. (G) Immunoblot of fly heads expressing Rh1 TMD1-5-V5 in Xport-A heterozygote (Xport-A¹/TM6B) or homozygous mutant flies (Xport-A¹/Xport-A¹). Extracts were untreated (–) or treated (+) with either Endo-H (lanes 2 and 5) or PNGase F enzyme (lanes 3 and 6). Each lane contains ~2,5 fly heads.

Source data are available online for this figure.

TRP contains 6 TMDs and a cytoplasmic N-terminus, which does not conform to the currently elucidated criteria for EMC client candidacy. An outstanding question is whether such non-canonical membrane protein clients are in fact engaged by the EMC for their biogenesis and if so, how? Several studies have reported the loss of multi-pass membrane proteins with loss of EMC functionality (Shurtleff *et al*, 2018; Tian *et al*, 2019; Miller-Vedam *et al*, 2020). Often, these studies correlate EMC-dependence with abundance changes at steady-state, rather than monitoring EMC-dependent biogenesis directly. Consequently, it remains possible that loss of some of these putative EMC clients will occur indirectly, as we have

demonstrated for Rh1 and TRP through Xport-A. Moreover, metabolic changes arising from disruption to EMC-dependent processes, such as sterol regulation, may also indirectly impact protein levels post-translationally through changes in their intrinsic stability, or via homeostatic mechanisms linked to transcription. Care must be exercised when interpreting EMC-dependent biogenesis of complex multi-pass clients to ensure that, in fact, what is observed is a direct impact linked to TMD engagement.

Studies from the Weissman lab identified features within the EMC structure that differentially impact TA protein clients when compared to multi-pass membrane proteins including TMEM97, a 4-

TMD protein with a similar cytoplasmic N-terminal topology to TRP (Miller-Vedam *et al*, 2020). One interpretation is that EMC may be able to handle distinct classes of clients through different features. Miller-Vedam and colleagues proposed that the EMC may function not only as an insertase for TA proteins, but also as a “holdase” factor, that participates in the biogenesis of a wider class of polytopic membrane proteins via distinct mechanisms, which may also include the recruitment of client-specific chaperones (Miller-Vedam *et al*, 2020). It will be important to determine whether the impact of EMC on TRP is fully indirect, through its impact on Xport-A, or whether TRP also engages the “holdase” function of EMC. The latter case could also involve recruitment of Xport-A to the EMC, to serve as a client-specific chaperone for Rh1/TRP, to aid in their maturation and/or release from the EMC and subsequent trafficking. Clearly, the biogenesis of membrane proteins via the EMC has far-reaching impact on organismal physiology and defining precisely the protein clients of EMC is indispensable to understand the selectivity of this complex.

Materials and Methods

Prediction of TA proteins in *Drosophila* proteome

The *Drosophila melanogaster* proteome (UP000000803, release 2018_10_26) was downloaded from the UniProt website (Bateman, 2019). Canonical forms of protein sequences longer than 49 amino acids (AAs) and shorter than 6,001 AAs were selected. Topology (i.e., localisation of TMDs and non-membrane regions) and presence of the signal peptide were predicted for each protein using the PolyPhobius (Käll *et al*, 2005) predictor implemented within the TOPCONS consensus predictor (Tsirigos *et al*, 2015). The presence of the mitochondrial targeting peptide was predicted for each protein using TargetP 1.1 (Emanuelsson *et al*, 2007). Proteins without predicted signal and mitochondrial targeting peptides, lacking the keywords “SIGNAL” and “TRANSIT” in their UniProt annotation, and containing only a single predicted TMD localised close to the C-terminus (i.e., followed by 35 or fewer flanking AAs) were selected. All thus selected protein sequences were analysed using the DeepLoc (Almagro Armenteros *et al*, 2017) cellular localisation predictor in order to further filter out soluble proteins. The TMD hydrophobicity was determined using the transmembrane tendency values for individual amino acids as defined by Zhao & London (Zhao & London, 2006). The C-terminal tail charge was calculated by adding +1 for arginine and lysine residues and –1 for aspartic and glutamic acid residues. The prediction of TA proteins was validated using experimentally identified proteins (Guna *et al*, 2018; Coy-Vergara *et al*, 2019). Characterisation of the distribution of cell localisations and biophysical features was performed in GraphPad Prism v.9 and significance was evaluated using the Kolmogorov–Smirnov test.

Fly stocks and crosses

Flies and crosses were raised with standard cornmeal, at 25°C under 12 h light/12 h dark cycles. Fly stocks used were obtained from multiple sources and are listed in Appendix Tables S2–S4.

To determine if expression of predicted TA proteins was dependent on EMC3, fly stocks carrying C-terminally HA-tagged

constructs on the third chromosome (obtained from FlyOrf – Zurich ORFeome Project) were crossed with flies with an EMC3 mutant allele EMC3^{Δ4}FRT40A (Satoh *et al*, 2015) on the second chromosome. The resulting flies (w; EMC3^{Δ4}FRT40A; UAS-TA-HA) were then crossed with eyFLP, GMRGAL4; ubiGFPFRT40A to obtain EMC3^{Δ4} mosaic eye imaginal discs, expressing the predicted TA proteins. In the case of VAP33A, hid and Na⁺K⁺ATPase α -subunit, there was no need to express tagged fly lines, as these genes are endogenously expressed in eye imaginal discs and antibodies were available.

Immunostaining and imaging

Larval eye imaginal discs and adult retina were dissected in 1× PBS, fixed in 4% PFA (paraformaldehyde) at room temperature (15 min for eye imaginal discs, 30 min for adult retina) and washed three times in PBT (1× PBS + 0.3% Triton X-100), 10 min each. For eye imaginal discs, primary antibodies were diluted in blocking buffer (1× PBS, 0.1% TX-100, 0.1% BSA, 250 mM NaCl) and for adult retina, primary antibodies were diluted in 5% Fetal Calf Serum in PBT. Primary antibody incubations were performed overnight at 4°C under gentle agitation. Primary antibodies were as follow: mouse anti-ELAV (1:50) (9F8A9, Developmental Studies Hybridoma Bank (DSHB)), rat anti-ELAV (1:50) (7E8A10, DSHB), rat anti-HA (1:400) (7C9, Chromotek), mouse anti-Rh1 (1:50) (4C5, DSHB), mouse anti-Na⁺K⁺ATPase α subunit (1:25) (A5-C, DSHB), rabbit anti-VAP33A (1:50—kind gift of Hugo Bellen), guinea pig anti-hid (kind gift from Hyung Don Ryoo), rabbit anti-HA (1:40) (9110, Abcam), mouse anti-TRP (1:25) (Mab83F6, DSHB). Samples were washed three times with PBT and incubated with appropriate secondary antibodies (Jackson Immuno Research) for 2 h at room temperature. Control staining of actin in the rhabdomeres of adult retina was performed with Phalloidin-FITC (1:500) (Abcam 235137). After rinsing three times with PBT, samples were mounted in Vectashield (Vector Laboratories). Adult eye samples were mounted in a bridge formed by two coverslips to prevent the samples from being crushed and analysed on a Zeiss LSM 880 confocal microscope. Larval eye imaginal discs were analysed on a Leica SP5Live confocal microscope. Adult testis were dissected in 1× PBS and fixed in 4% PFA overnight at 4°C under gentle agitation. Following this, samples were washed three times in PBS, 5 min each and then treated with PBT at room temperature for 30 min. After three more washes with PBS (5 min each), testis were incubated with rabbit anti-cleaved caspase 3 (1:200) (Asp175, Cell Signaling) diluted in 0.1% PBT, overnight at 4°C. Samples were washed three times with PBS, 5 min each, and incubated with anti-rabbit Cy3 (1:200) (Jackson Immuno Research). After three more washes with PBS (5 min each), samples were incubated with DAPI, diluted in 0.1% PBT for 10 min. After rinsing three more times with PBS, samples were mounted in Vectashield and image acquisition was performed in Leica SP5Live. For measurement of seminal vesicle size, testis were stained with DAPI, as described above and image acquisition was performed in Leica SP5Live. Imaging was performed at the widest portion of the seminal vesicle and area measurement was performed in Fiji. Characterisation of distribution of seminal vesicle size was performed in GraphPad Prism v.9 and significance was determined by Welch’s *t*-test.

Quantification of protein expression in EMC3^{A4} mutant clones

Quantification was executed in Fiji (Schindelin *et al*, 2012). Maximum intensity projections were performed on the raw confocal data to visualise EMC3^{A4} mutant clones. The three coloured images were split into single colour images. Channel 1 corresponded to ubiGFP, in which homozygous mutant clones were identified by the absence of fluorescence. Channel 2 corresponded to the fluorescence signal for the protein of interest, while channel 3, which showed ELAV staining, marked the photoreceptor cells. Segmentation was first performed on channel 3 to define the GMRGAL4 domain, and then on channel 1 to highlight patches with no detectable ubiGFP fluorescence, which coincided with EMC3^{A4} homozygous mutant cells. Both segmentations were performed using the Otsu thresholding method (Otsu, 1979). Following segmentation, the mathematical process “AND” was performed to intersect mutant patches delimited in the second segmentation with the GMRGAL4 domain identified in the first segmentation. EMC3^{A4} mutant patches in the GMRGAL4 domain were defined as ROIs. Mean grey values for the ROIs in channel 2 were measured (EMC3^{A4} mean) and compared to mean grey values of WT patches of comparable area in channel 2 (WT mean). A ratio of fluorescence intensity in EMC3^{A4} mutant cells/WT cells was calculated for each protein. For quantification, at least three mutant patches were quantified per eye imaginal disc, and at least three eye imaginal discs derived from distinct flies were used. Significance was evaluated using the Welch’s *t*-test in GraphPad Prism v.9 software.

Generation of transgenic flies

To generate transgenic flies expressing HA tagged Xport-A we PCR amplified the full open reading frame of Xport-A from plasmid pAC5.1-FLAG::XPORT-A (kind gift of Craig Montell). For N-terminally tagged Xport-A, we used the following primers: 5'-CCGATTACGCCAAGCCGAAGAAATCGGCC-3' and 5'-CGCAGATCTGTTAACGAATTCTTACTGCTGATGCTCCTCGC-3'. For C-terminally tagged Xport-A we used the following primers: 5'-GAATAGGGAATTGGGAATTCATG AAGCCGAAGAAATCGGCC-3' and 5'-TCAGGGACGTCGTA CGGTACTGCTGATGCTCCTCGC GAAAG-3'. For amplification of 3XHA tag, we PCR amplified 3XHA with following primers: 5'-TGAATAGGGAATTGGGAATTCATGTAC CCGTACGACGTCCCTGA-3' and 5'-TCTTCGGCTTGGC GTAATCC GGCACATCA-3' for HA-Xport-A. For PCR amplification of 3XHA intended for Xport-A-HA, we used the following primers: 5'-GAAAGCTTTCGCGAGGAGCATCAGCA GTACCCGTACGACGTCCC TGA-3' and 5'-CGCAGATC TGTTAACGAATTCTTAGCCGGCGTA ATCCGGCACATCA-3'. After amplification of Xport-A and 3XHA inserts, we proceeded to perform a Gibson assembly[®] (New England Biolabs) with plasmid pUASTattb (previously linearised with EcoRI).

Xport-A2L and XportA-4L constructs were made by mutating hydrophilic AAs to Leucine, using KOD polymerase site-directed mutagenesis (Merck Millipore). Xport-A4L insert was then amplified by PCR with primers listed above and Gibson assembly was used to create N-terminal and C-terminal HA tagged pUASTattb constructs. Xport-A2L insert was also amplified by PCR with primers listed above and Gibson assembly was used to create N-terminal HA tagged pUASTattb constructs. The resulting

constructs were inserted into the *atp2* site by PhiC31 integrase mediated transgenesis at the Champalimaud Foundation transgenics facility.

For the generation of flies expressing Rh1TMD1-5-N196I-V5, we fused the DNA sequence encoding the Rh1 TMD1-5 fragment with N196 mutagenised to I (M¹- N196I-V²⁴¹) to Rh1 C-tail-V5-fusion (H³³³-A³⁷³-WSHPQFEKGGGRKPIPPLLGLDST*). We PCR amplified the plasmid pUASTattb-Rh1 (kind gift of Hyung Don Ryoo) with primers PFpuast-Rh1TMD1 (5' actctgaatagggaattgggaattcgc-caccatggagagcttgcagtagca 3') and PR-Rh1TMD5-Cterm (5' aggcaatcttggccaggccagcgaatggctatcgcc 3'), generating insert 1. Then, we ordered a geneblock (IDT) containing the Rh1 sequence I¹⁶³-N196I-V²⁴¹ fused to the Rh1 C-tail-V5 fusion. The geneblock was amplified with primers PF Rh1-TMD5-Cterm (5' attccgctggc-ctgggcaagattg 3') and PR-V5-puast (5' gccgcagatctgtaacgaatttaggt-gtattccagggcccag 3'), creating insert 2. After amplification of insert 1 and insert 2, we performed Gibson assembly[®] (New England Biolabs) with plasmid pUASTattb (previously linearised with EcoRI). The construct was inserted into the *atp40* site by PhiC31 integrase mediated transgenesis at the Champalimaud Foundation transgenics facility.

Cell culture

U2OS Flp-In[™] TRex[™] cell lines described previously (Volkmar *et al*, 2019) were maintained in Dulbecco’s Modified Eagle Medium (Biowest) + 10% v/v fetal bovine serum (FBS) (Biowest) + L-glutamine (2 mM) (GRiSP) + 1% v/v Penicillin-Streptomycin (Biowest) in 5% CO₂ at 37°C. Stable expression cell lines, generated by flippase mediated site-specific integration, were continuously cultured in 100 µg/ml hygromycin B (Merck Millipore). Cells containing stably expressed tetracycline-induced constructs were cultured in tetracycline-free FBS (Biowest), 100 µg/ml hygromycin, with their expression induced by addition of 1 µg/ml doxycycline (Sigma Aldrich).

Plasmids and expression constructs

Xport-A and Xport-A4L dual fluorescent reporters were generated by first amplifying the TMD and flanking residues of Xport-A (AFEMMKLVFVANTIMLIVTMAWPHIKEQFYM) and Xport-A4L (AFEMMKLVFVALLIMLIVLMAWPLIKEQFYM) using the primers PFmcherry-xportTMD (GGCGGCATGGACGAGCGTTACAAGC-CATTTGAAATGATGAACTC) and PRmcherry-xportTMD (TTATGATCAGTTATCTAGATCCGTTTACATGTAGAATTGCTCCTTGAT). Reporter plasmids were constructed from BamHI-linearised, dephosphorylated pcDNA5/FRT/TO-GFP-P2A-mcherry vector (kind gift from Manu Hegde, LMB-Cambridge) using Gibson assembly[®] (New England Biolabs). The SQS fluorescent reporter GFP-P2A-mcherry-SQS has been reported previously (Guna *et al*, 2018). TMD insertion reporters pcDNA5/FRT/TO-HA:SQS_{opsin} and pcDNA5/FRT/TO-HA:SQS-Sec61βTMD^{opsin} have been reported previously (Volkmar *et al*, 2019). To generate XportATMD^{opsin} (pcDNA5/FRT/TO-HA:SQS-XportATMD^{opsin}) and hydrophobic TMD variants (1L/2L/3L/4L), geneblocks (IDT) containing each TMD sequence fused to the opsin tag were purchased. Each gene block contained flanking restriction sites for BamHI and XhoI that enabled subcloning into linearised pcDNA5/FRT/TO-HA:SQS.

Flow cytometry

Analysis of protein post-translational stability was performed according to described methods (Guna *et al*, 2018). Cells were transfected with fluorescent reporter constructs (1 µg total DNA/well, six well plate) using GenJet (SignaGen Laboratories) according to manufacturer's instructions. The amount of fluorescent reporter for each protein of interest was titrated according to transfection efficiency and a control plasmid was co-transfected in order to maintain the total amount of DNA (1 µg/well). The U2OS FlpIn Trex EMC5KO rescue cell lines were cultured in the presence of doxycycline (1 µg/ml) for 24 h prior to transfection, to rescue EMC5 expression. After transfection, cells were trypsinised, washed twice with PBS + 2%FCS and stained with DAPI (to determine cell viability). Flow cytometry was performed on a BD LSR Fortessa ×20 instrument, where 20,000 RFP-positive cells were collected. Data analysis was performed in FlowJo (v10). For quantification, cells were first gated for GFP (translation reporter) and mean RFP and GFP fluorescence intensities were determined. Then, RFP:GFP ratios were calculated and normalised to the ratio observed in WT cells.

Transient transfection of TMD insertion reporters

1 × 10⁶ cells/6 cm² tissue culture plate were transfected with TMD insertion reporters (2.5 µg total DNA/6 cm² plate) using GenJet (SignaGen Laboratories) according to manufacturer's instructions. The following day, cells were lysed.

Immunoblotting of mammalian cells

Cells were washed twice in ice-cold PBS and lysed in TX-100 lysis buffer (50 mM Tris-HCl pH 7.4, 150 mM NaCl, 1% Triton X-100, 5 mM EDTA and protease inhibitors). Following incubation on ice (10 min), lysates were centrifuged (top speed, 10 min, 4°C). Protein concentrations were determined by Bradford and protein denaturation was performed by adding 3× LDS buffer + DTT and incubating the samples at 65°C (15 min). After denaturation, samples were digested with PNGaseF (New England Biolabs) for 2 h at 37°C, according to manufacturer's instructions. Samples were fractionated by SDS-PAGE, transferred to PVDF membranes (Amersham Hybond) and probed with following antibodies: mouse anti-HA-HRP (1:1,000) (12013819001, Roche) rabbit anti-EMC6 (1:300) (84902, Abcam), rabbit anti-actin (1:2,000) (8227, Abcam), rat anti-tubulin (1:1,000) (YL1-2 clone, homemade), rabbit anti-EMC3 (1:200) (365903, Santa Cruz), rabbit anti-EMC5 (1:500) (122202, Abcam).

Immunoblotting of fly heads

Heads from 1-day old flies were homogenised in 2× LDS buffer + DTT with a pellet pestle, and then diluted with MilliQ water. Protein denaturation was performed by incubating extracts at 65°C (15 min). After denaturation, samples were digested with Endo-H (New England Biolabs) or PNGase F (New England Biolabs) for 2 h at 37°C, according to manufacturer's instructions. Samples were fractionated by SDS-PAGE, transferred to PVDF membranes (Amersham Hybond) and probed with the following antibodies: mouse anti-V5 (1:1,000) (R960-25, Invitrogen), mouse anti-TRP (1:300) (Mab83F6,

DSHB), mouse anti-Rh1 (1:200) (4C5, DSHB), rat anti-Xport-A antibody (1:400) (kind gift of Craig Montell), and mouse anti-tubulin (1:1,000) (AA4.3, DSHB).

Immunoblotting of fly eyes

Flies were collected and placed in acetone overnight at −20°C. The following day, flies were placed on filter paper to dry (5 min), and then heads were cut dry using a dissecting knife. Then, eyes were easily dissected and placed inside eppendorf tubes containing 10 µl of 2× LDS buffer + DTT, on ice. Eyes were homogenised with a pellet pestle and protein denaturation was performed by incubating extracts at 65°C (15 min). Samples were fractionated by SDS-PAGE, transferred to PVDF membranes (Amersham Hybond) and probed with the following antibodies: rat anti-EMC3 (1:250) (kind gift from Akiko Satoh), rat anti-Xport-A antibody (1:400) (kind gift from Craig Montell), mouse anti-TRP (1:300) (Mab83F6, DSHB), mouse anti-Rh1 (1:200) (4C5, DSHB), and mouse anti-tubulin (1:1,000) (AA4.3, DSHB). For each genotype, a minimum of 30 eyes were dissected.

Fertility assay

To examine fertility, individual adult males (3-days old) were mated to three wild-type virgin females in separate vials. All RNAi lines were expressed with bam-GAL4 driver. For each RNAi line, thirty individual males were mated to virgin females. The females were transferred after 7 days at 25°C to fresh vials. Progeny from the original vial and the first transfer vial were counted. Characterisation of distribution of progeny/female/day was performed in GraphPad Prism v.9 and significance was determined by Welch's *t*-test.

Data availability

The macro method developed for the quantification of protein expression in EMC3^{A4} mutant clones can be found on Github (<https://github.com/zserrado-marques/Quantification-of-protein-expression-inside-dark-patches>).

Expanded View for this article is available online.

Acknowledgements

We thank the flow cytometry facility at IGC, the microscopy facility at IGC (more specifically José Marques), the microscopy facility at ITQB-NOVA, the fly facility from IGC and the transgenics facility at Champalimaud Foundation—Centre for the Unknown. We thank the Developmental Studies Hybridoma Bank (DSHB) at the University of Iowa for antibodies and the Bloomington Drosophila Stock Centre for fly stocks. We thank Craig Montell for flies, plasmids and antibodies, Akiko Satoh for flies and antibodies, and Manu Hegde for plasmids. We also acknowledge Norbert Volkmar and Miguel Cavadas for discussions and suggestions, Nansi Jo Colley and Steve Britt for antibodies, Hugo Bellen for VAP33A antibody, Hyung Don Ryoo for UAS-Rh1 flies and hid antibody, Stephen High for cells and Paulo Navarro Costa for flies. We thank Sebastien Alfaiate for help with figure design. The project leading to these results was funded by 'la Caixa' Foundation, under the agreement <LCR/PR/HR17/52150018>.

Author contributions

Research design: all authors. TA protein prediction was done by DJ and KS. All experiments were performed by CJG, except the *Drosophila* male fertility experiments (LCV). Paper writing and editing: all authors.

Conflict of interest

The authors declare that they have no conflict of interest.

References

- Almagro Armenteros JJ, Sønderby CK, Sønderby SK, Nielsen H, Winther O (2017) DeepLoc: prediction of protein subcellular localization using deep learning. *Bioinformatics* 33: 3387–3395
- Arama E, Agapite J, Steller H (2003) Caspase activity and a specific cytochrome C are required for sperm differentiation in *Drosophila*. *Dev Cell* 4: 687–697
- Bagchi P, Inoue T, Tsai B (2016) EMC1-dependent stabilization drives membrane penetration of a partially destabilized non-enveloped virus. *eLife* 5: 1–23
- Bagchi P, Torres M, Qi L, Tsai B (2020) Selective EMC subunits act as molecular tethers of intracellular organelles exploited during viral entry. *Nat Commun* 11: 1–15
- Bai L, You Q, Feng X, Kovach A, Li H (2020) Structure of the ER membrane complex, a transmembrane-domain insertase. *Nature* 584: 475–478
- Barrows NJ, Anglero-Rodriguez Y, Kim B, Jamison SF, Le Sommer C, McGee CE, Pearson JL, Dimopoulos G, Ascano M, Bradrick SS et al (2019) Dual roles for the ER membrane protein complex in flavivirus infection: viral entry and protein biogenesis. *Sci Rep* 9: 1–16
- Bateman A (2019) UniProt: A worldwide hub of protein knowledge. *Nucleic Acids Res* 47: D506–D515
- Borgese N, Colombo S, Pedrazzini E (2003) The tale of tail-anchored proteins: coming from the cytosol and looking for a membrane. *J Cell Biol* 161: 1013–1019
- Brambillasca S, Yabal M, Soffientini P, Stefanovic S, Makarow M, Hegde RS, Borgese N (2005) Transmembrane topogenesis of a tail-anchored protein is modulated by membrane lipid composition. *EMBO J* 24: 2533–2542
- Chen YN, Wu CH, Zheng Y, Li JJ, Wang JL, Wang YF (2015a) Knockdown of ATPsyn-b caused larval growth defect and male infertility in *Drosophila*. *Arch Insect Biochem Physiol* 88: 144–154
- Chen Z, Chen HC, Montell C (2015b) TRP and rhodopsin transport depends on dual XPORT ER chaperones encoded by an operon. *Cell Rep* 13: 573–584
- Chitwood PJ, Juszkiwicz S, Guna A, Shao S, Hegde RS (2018) EMC is required to initiate accurate membrane protein topogenesis. *Cell* 175: 1–13
- Chitwood PJ, Hegde RS (2019) The role of EMC during membrane protein biogenesis. *Trends Cell Biol* 29: 1–14
- Chiu CF, Ghanekar Y, Frost L, Diao A, Morrison D, McKenzie E, Lowe M (2008) ZFPL1, a novel ring finger protein required for cis-Golgi integrity and efficient ER-to-Golgi transport. *EMBO J* 27: 934–947
- Christianson JC, Olzmann JA, Shaler TA, Sowa ME, Bennett EJ, Richter CM, Tyler RE, Greenblatt EJ, Harper JW, Kopito RR (2011) Defining human ERAD networks through an integrative mapping strategy. *Nat Cell Biol* 14: 93–105
- Coelho JPL, Stahl M, Bloemeke N, Meighen-Berger K, Alvira CP, Zhang Z-R, Sieber SA, Feige MJ (2019) A network of chaperones prevents and detects failures in membrane protein lipid bilayer integration. *Nat Commun* 10: 1–10
- Costello JL, Castro IG, Camões F, Schrader TA, McNeill D, Yang J, Giannopoulou E-A, Gomes S, Poggenberg V, Bonekamp NA et al (2017) Predicting the targeting of tail-anchored proteins to subcellular compartments in mammalian cells. *J Cell Sci* 130: 1675–1687
- Coy-Vergara J, Rivera-Monroy J, Urlaub H, Lenz C, Schwappach B (2019) A trap mutant reveals the physiological client spectrum of TRC40. *J Cell Sci* 132: jcs230094
- Emanuelsson O, Brunak S, von Heijne G, Nielsen H (2007) Locating proteins in the cell using TargetP, SignalP and related tools. *Nat Protoc* 2: 953–971
- Fagerberg L, Jonasson K, Von Heijne G, Uhlén M, Berglund L (2010) Prediction of the human membrane proteome. *Proteomics* 10: 1141–1149
- Guna A, Hegde RS (2018) Transmembrane domain recognition during membrane protein biogenesis and quality control. *Curr Biol* 28: R498–R511
- Guna A, Volkmar N, Christianson JC, Hegde RS (2018) The ER membrane protein complex is a transmembrane domain insertase. *Science* 359: 470–473
- Harel T, Yesil G, Bayram Y, Coban-Akdemir Z, Charng W-L, Karaca E, Al Asmari A, Eldomery M, Hunter J, Jhangiani S et al (2016) Monoallelic and biallelic variants in EMC1 identified in individuals with global developmental delay, hypotonia, scoliosis, and cerebellar atrophy. *Am J Hum Genet* 98: 562–570
- Hegde RS, Keenan RJ (2011) Tail-anchored membrane protein insertion into the endoplasmic reticulum. *Nat Rev Mol Cell Biol* 12: 787–798
- Hiramatsu N, Tago T, Satoh T, Satoh AK (2019) ER membrane protein complex is required for the insertions of late-synthesized transmembrane helices of Rh1 in *Drosophila* photoreceptors. *Mol Biol Cell* 30: 2890–2900
- Janer A, Prudent J, Paupe V, Fahiminiya S, Majewski J, Sgarioto N, Des RC, Forest A, Lin Z, Gingras A et al (2016) SLC 25 A 46 is required for mitochondrial lipid homeostasis and cristae maintenance and is responsible for Leigh syndrome. *EMBO Mol Med* 8: 1–20
- Jonikas MC, Collins SR, Denic V, Oh E, Quan EM, Schmid V, Weibezahn J, Schwappach B, Walter P, Weissman JS et al (2009) Comprehensive characterization of genes required for protein folding in the endoplasmic reticulum. *Science* 323: 1693–1697
- Käll L, Krogh A, Sonnhammer ELL (2005) An HMM posterior decoder for sequence feature prediction that includes homology information. *Bioinformatics* 21: 251–257
- Katanosaka K, Tokunaga F, Kawamura S, Ozaki K (1998) N-Linked glycosylation of *Drosophila* rhodopsin occurs exclusively in the amino-terminal domain and functions in rhodopsin maturation. *FEBS Lett* 424: 149–154
- Kriechbaumer V, Shaw R, Mukherjee J, Bowsler CG, Harrison AM, Abell BM (2009) Subcellular distribution of tail-anchored proteins in arabidopsis. *Traffic* 10: 1753–1764
- Kutay U, Hartmann E, Rapoport TA (1993) A class of membrane proteins with a C-terminal anchor. *Trends Cell Biol* 3: 72–75
- Lahiri S, Chao JT, Tavassoli S, Wong AKO, Choudhary V, Young BP, Loewen CJR, Prinz WA (2014) A conserved endoplasmic reticulum membrane protein complex (EMC) facilitates phospholipid transfer from the ER to mitochondria. *PLoS Biol* 12: e1001969
- Lakshminarayan R, Phillips BP, Binnian IL, Gomez-Navarro N, Escudero-Urquijo N, Warren AJ, Miller EA (2020) Pre-emptive quality control of a misfolded membrane protein by ribosome-driven effects. *Curr Biol* 30: 854–864
- Li Y, Zhao Y, Hu J, Xiao J, Qu L, Wang Z, Ma D, Chen Y (2013) A novel ER-localized transmembrane protein, EMC6, interacts with RAB5A and regulates cell Autophagy. *Autophagy* 9: 150–163

- Lin DL, Inoue T, Chen YJ, Chang A, Tsai B, Tai AW (2019) The ER membrane protein complex promotes biogenesis of dengue and Zika virus non-structural multi-pass transmembrane proteins to support infection. *Cell Rep* 27: 1666–1674
- Louie RJ, Guo J, Rodgers JW, White R, Shah NA, Pagant S, Kim P, Livstone M, Dolinski K, McKinney BA et al (2012) A yeast phenomic model for the gene interaction network modulating CFTR- Δ F508 protein biogenesis. *Genome Med* 4: 103
- Ma Z, Liu Z, Huang X (2010) OSBP- and FAN-mediated sterol requirement for spermatogenesis in *Drosophila*. *Development* 137: 3775–3784
- Mariappan M, Mateja A, Dobosz M, Bove E, Hegde RS, Keenan RJ (2011) The mechanism of membrane-associated steps in tail-anchored protein insertion. *Nature* 477: 61–69
- Mateja A, Paduch M, Chang HY, Szydłowska A, Kosiakoff AA, Hegde RS, Keenan RJ (2015) Structure of the Get3 targeting factor in complex with its membrane protein cargo. *Science* 347: 1152–1155
- Miller-Vedam LE, Bräuning B, Popova KD, Schirle Oakdale NT, Bonnar JL, Prabu JR, Boydston EA, Sevillano N, Shurtleff MJ, Stroud RM et al (2020) Structural and mechanistic basis of the EMC-dependent biogenesis of distinct transmembrane clients. *eLife* 9: 1–47
- O'Donnell JP, Phillips BP, Yagita Y, Juszkiewicz S, Wagner A, Malinverni D, Keenan RJ, Miller EA, Hegde RS (2020) The architecture of EMC reveals a path for membrane protein insertion. *eLife* 9: 1–30
- O'Tousa JE (1992) Requirement of N-linked glycosylation site in *Drosophila* rhodopsin. *Vis Neurosci* 8: 385–390
- Otsu N (1979) A threshold selection method from Gray-level histograms. *IEEE Trans Syst Man Cybern* 9: 62–66
- Pleiner T, Tomaleri GP, Januszyk K, Inglis AJ, Hazu M, Voorhees RM (2020) Structural basis for membrane insertion by the human ER membrane protein complex. *Science* 369: 433–436
- Rao M, Okreglak V, Chio US, Cho H, Walter P, Shan S-O (2016) Multiple selection filters ensure accurate tail-anchored membrane protein targeting. *eLife* 5: 1–24
- Richard M, Boulin T, Robert VJP, Richmond JE, Bessereau J-L (2013) Biosynthesis of ionotropic acetylcholine receptors requires the evolutionarily conserved ER membrane complex. *Proc Natl Acad Sci USA* 110: E1055–E1063
- Rosenbaum EE, Brehm KS, Vasiljevic E, Liu CH, Hardie RC, Colley NJ (2011) XPORT-dependent transport of TRP and rhodopsin. *Neuron* 72: 602–615
- Rosenbaum EE, Vasiljevic E, Brehm KS, Colley NJ (2014) Mutations in four glycosyl hydrolases reveal a highly coordinated pathway for rhodopsin biosynthesis and N-glycan trimming in *Drosophila melanogaster*. *PLoS Genet* 10: e1004349
- Satoh T, Ohba A, Liu Z, Inagaki T, Satoh AK (2015) dPob/EMC is essential for biosynthesis of rhodopsin and other multi-pass membrane proteins in *Drosophila* photoreceptors. *eLife* 4: 1–21
- Savidis G, McDougall WM, Meraner P, Perreira JM, Portmann JM, Trincucci G, John SP, Aker AM, Renzette N, Robbins DR et al (2016) Identification of Zika virus and dengue virus dependency factors using functional genomics. *Cell Rep* 16: 232–246
- Schindelin J, Arganda-Carreras I, Frise E, Kaynig V, Longair M, Pietzsch T, Preibisch S, Rueden C, Saalfeld S, Schmid B et al (2012) Fiji: an open-source platform for biological-image analysis. *Nat Methods* 9: 676–682
- Schuldiner M, Metz J, Schmid V, Denic V, Rakwalska M, Schmitt HD, Schwappach B, Weissman JS (2008) The GET complex mediates insertion of tail-anchored proteins into the ER membrane. *Cell* 134: 634–645
- Shen X, Kan S, Hu J, Li M, Lu G, Zhang M, Zhang S, Hou Y, Chen Y, Bai Y (2016) EMC6/TMEM93 suppresses glioblastoma proliferation by modulating autophagy. *Cell Death Dis* 7: e2043
- Shurtleff MJ, Itzhak DN, Hussmann JA, Schirle Oakdale NT, Costa EA, Jonikas M, Weibezahn J, Popova KD, Jan CH, Sinitcyn P et al (2018) The ER membrane protein complex interacts cotranslationally to enable biogenesis of multipass membrane proteins. *eLife* 7: 1–23
- Stefanovic S, Hegde RS (2007) Identification of a targeting factor for posttranslational membrane protein insertion into the ER. *Cell* 128: 1147–1159
- Stefer S, Reitz S, Wang F, Wild K, Pang Y-Y, Schwarz D, Bomke J, Hein C, Löhner F, Bernhard F et al (2011) Structural basis for tail-anchored membrane protein biogenesis by the Get3-receptor complex. *Science* 333: 758–762
- Tang X, Snowball JM, Xu Y, Na C-L, Weaver TE, Clair G, Kyle JE, Zink EM, Ansong C, Wei W et al (2017) EMC3 coordinates surfactant protein and lipid homeostasis required for respiration. *J Clin Invest* 127: 4314–4325
- Taylor MR, Kikkawa S, Diez-Juan A, Ramamurthy V, Kawakami K, Carmeliet P, Brockerhoff SE (2005) The zebrafish pob gene encodes a novel protein required for survival of red cone photoreceptor cells. *Genetics* 170: 263–273
- Tian S, Wu Q, Zhou B, Choi MY, Ding B, Yang W, Dong M (2019) Proteomic analysis identifies membrane proteins dependent on the ER membrane protein complex. *Cell Rep* 28: 2517–2526
- Tsirigos KD, Peters C, Shu N, Käll L, Elofsson A (2015) The TOPCONS web server for consensus prediction of membrane protein topology and signal peptides. *Nucleic Acids Res* 43: W401–W407
- Volkmar N, Thezenas ML, Louie SM, Juszkiewicz S, Nomura DK, Hegde RS, Kessler BM, Christianson JC (2019) The ER membrane protein complex promotes biogenesis of sterol-related enzymes maintaining cholesterol homeostasis. *J Cell Sci* 132: jcs223453
- Volkmar N, Christianson JC (2020) Squaring the EMC – how promoting membrane protein biogenesis impacts cellular functions and organismal homeostasis. *J Cell Sci* 133: 1–14
- Wallin E, Von Heijne G (1998) Genome-wide analysis of integral membrane proteins from eubacterial, archaean, and eukaryotic organisms. *Protein Sci* 7: 1029–1038
- Wang F, Brown EC, Mak G, Zhuang J, Denic V (2010) A chaperone cascade sorts proteins for posttranslational membrane insertion into the endoplasmic reticulum. *Mol Cell* 40: 159–171
- Webel R, Menon I, Tousa JEO, Colley NJ (2000) Role of asparagine-linked oligosaccharides in rhodopsin maturation and association with its molecular chaperone, NinaA. *J Biol Chem* 275: 24752–24759
- Wideman JG (2015) The ubiquitous and ancient ER membrane protein complex (EMC): tether or not? *F1000Res* 4: 624
- Xiong L, Zhang L, Yang Y, Li N, Lai W, Wang F, Zhu X, Wang T (2020) ER complex proteins are required for rhodopsin biosynthesis and photoreceptor survival in *Drosophila* and mice. *Cell Death Differ* 27: 646–661
- Zhao G, London E (2006) An amino acid “transmembrane tendency” scale that approaches the theoretical limit to accuracy for prediction of transmembrane helices: Relationship to biological hydrophobicity. *Protein Sci* 15: 1987–2001
- Zhou Y, Wu F, Zhang M, Xiong Z, Yin Q, Ru Y, Shi H, Li J, Mao S, Li Y et al (2018) EMC 10 governs male fertility via maintaining sperm ion balance. *J Mol Cell Biol* 6: 503–514